

1 **Aerosolizable plasmid DNA dry powders engineered by thin-film freezing**

2
3
4 Haiyue Xu,¹ Chaeho Moon,¹ Sawittree Sahakijpijarn,² Huy M. Dao¹, Riyad F. Alzhrani¹,
5 Jie-liang Wang¹, Robert O. Williams III^{1*} and Zhengrong Cui^{1*}
6

7
8 ¹ Division of Molecular Pharmaceutics and Drug Delivery, College of Pharmacy,
9 The University of Texas at Austin, Austin, TX, 78712, USA
10

11 ² TFF Pharmaceuticals, Inc. Austin, TX, 78753, USA
12

13
14 * Correspondence should be sent to:

15 bill.williams@austin.utexas.edu or Zhengrong.cui@austin.utexas.edu
16
17
18
19
20
21
22
23
24
25
26
27
28
29
30
31

32 **ABSTRACT**

33

34 This study was designed to test the feasibility of using thin-film freezing (TFF) to
35 prepare aerosolizable dry powders of plasmid DNA (pDNA) for pulmonary delivery. Dry
36 powders of pDNA formulated with mannitol/leucine (70/30, w/w) at various of drug
37 loadings, solid contents, and solvents were prepared using TFF, their aerosol properties
38 (i.e., mass median aerodynamic diameter (MMAD) and fine particle fraction (FPF))
39 determined, and selected powders were used for further characterization. Of the nine
40 dry powders prepared, their MMAD values were about 1-2 μ m, with FPF values
41 (delivered) of 40-80%. The aerosol properties of the powders were inversely correlated
42 with the pDNA loading and the solid content in the pDNA solution before thin-film
43 freezing. Powders prepared with Tris-EDTA (TE) buffer or cosolvents (i.e., 1,4 dioxane
44 or t-butanol in water), instead of water, showed slightly reduced aerosol properties.
45 Ultimately, powders prepared with pDNA loading at 5% (w/w), 0.25% of solid content,
46 with or without TE were selected for further characterization due to their overall good
47 aerosol performance. The pDNA powders exhibited a porous matrix, crystalline
48 structure, with a moisture content of <2% (w/w). Agarose gel electrophoresis confirmed
49 the chemical integrity of the pDNA after it was subjected to TFF and after the TFF
50 powder was actuated. A cell transfection study confirmed the activity of the pDNA after
51 it was subjected to TFF. In conclusion, it is feasible to use TFF to produce aerosolizable
52 pDNA dry powder for pulmonary delivery, while preserving the integrity and activity of
53 the pDNA.

54

55 **KEYWORDS:** Freeze-drying, Nucleic acid, Powder, Pulmonary, Cell transfection

56

57

58

59

60

61

62

63 INTRODUCTION

64 The lung is an appealing target for administering nucleic acid-based products such as
65 plasmid DNA (pDNA) for vaccination by oral inhalation, due to the non-invasive nature
66 of pulmonary delivery and the vast and highly vascularized surface area of the lung [1,
67 2]. Moreover, pulmonary delivery of pDNA holds potential in treating various lung
68 diseases caused by gene mutations, such as cystic fibrosis, alpha-1 antitrypsin
69 deficiency, acute illnesses such as acute transplant rejection, as well as lung cancer [3-
70 6]. However, effective pulmonary administration of pDNA has been challenging. Only
71 aerosol droplets or particles with aerodynamic diameters in the range of 1 to 5 μm can
72 reach and contact bronchial and alveolar epithelial cells upon inhalation [7]. However,
73 pulmonary delivery of naked pDNA is challenging using traditional nebulizers, including
74 jet and ultrasonic nebulizers, due to the shear and cavitation stresses associated with
75 nebulization [8-10]. The collapse of air bubbles creates shock waves that can damage
76 the pDNA, with their tertiary structure changing from supercoiled to open circular (i.e.,
77 nicking form) and/or fragmented configurations (e.g., linear form or even small
78 fragments) [8-10]. The sensitivity of pDNA to shearing is strongly correlated with
79 plasmid length; plasmids of above 5 kb are significantly more sensitive to shear-induced
80 degradation than smaller plasmids [8, 11]. Unfortunately, the damage caused by
81 shearing can be consequential, causing the transfection efficiency of pDNA after
82 nebulization to decrease to 10% [12].

83
84 Pulmonary delivery of pDNA in a dry powder form by oral inhalation using a dry powder
85 inhaler (DPI) is an alternative method to nebulization of pDNA in liquid. However, dry
86 powder engineering technologies such as spray drying and spray freeze-drying that can
87 generate powders with good aerosol properties for lung delivery also involve
88 atomization of liquid by spraying, and the shear stress associated with the atomization
89 has proven damaging to pDNA [13, 14]. For example, Kuo and Hwang (2003) reported
90 that spray freeze-drying adversely affects the tertiary structure of pDNA, resulting in
91 linear form of DNA even in the presence of protective agents such as sucrose,
92 trehalose, or mannitol. The similar pDNA damage was also reported when the pDNA
93 was subjected to spray drying [15, 16].

94 Thin-film freezing (TFF) is an ultra-rapid freezing technology, which employs a
95 cryogenically cooled solid surface to freeze samples. Small droplets of liquid (~2 mm in
96 diameter) are dropped from above the surface. Upon impact, the droplet spreads and is
97 then frozen in 70-3000 milliseconds. Drying of the frozen thin films by lyophilization
98 generates powders often with desirable aerosol properties, due to their low-density,
99 large specific surface area, and brittle matrix nature [17-19]. TFF technology has been
100 used to prepare aerosolizable dry powders of small molecule drugs for pulmonary
101 delivery, such as tacrolimus, remdesivir, voriconazole, and niclosamide [20-25].
102 Recently, it has also been applied to large molecules such as monoclonal antibodies
103 and enzymes and particulates such as liposomes and small interfering RNA-solid lipid
104 nanoparticles [26-32]. Due to the low shear stress associated with TFF, using TFF to
105 prepare dry powders minimizes the detrimental effect from shear stress to large
106 molecules such as monoclonal antibodies and enzymes, as compared to spray freeze-
107 drying and spray drying [33].

108

109 In this study, two plasmids that encode β -galactosidase (β -gal) or green fluorescent
110 protein (GFP) were employed to study the feasibility of applying TFF to prepare
111 aerosolizable dry powders of plasmids. The pDNA powders were prepared with
112 mannitol and leucine (70:30, w/w) as excipients as powders prepared with this specific
113 excipient composition generally have good aerosol properties [34]. The effect of Tris-
114 EDTA (TE) buffer and co-solvents including 1,4-dioxane or *Tert*-butanol on the aerosol
115 performance properties of the resultant dry powders were also evaluated. Finally, the
116 integrity of pDNA after being subjected to thin-film freezing (TFF) and actuation using a
117 DPI device was tested using agarose gel electrophoresis and/or transfection of A549
118 human lung epithelial-like cells in culture.

119

120

121

122

123

124

125 **MATERIALS AND METHODS**

126

127 *Materials*

128 The β -galactosidase gene-encoding pDNA pCMV- β was from the American Type
129 Culture Collection (ATCC, Manassas, VA). It was constructed based on pUC19 plasmid
130 with a AMP^r gene, capable of expressing *E.coli* β -Gal under the control of different viral
131 promoters in mammalian cells [35]. The GFP expressing plasmid pVectOZ-GFP was
132 from OZbiosciences (San Diego, CA), which contains a modified human
133 cytomegalovirus (CMV) promoter and a KAN^r gene. DH5 α competent cells, LB broth,
134 cell extraction buffer and Lipofectamine 3000 reagent were from Invitrogen (Carlsbad,
135 CA). Plasmid Midiprep kit and Maxi kit were from QIAGEN (Valencia, CA). The 1,4-
136 dioxane, *tert*-butanol, TE buffer, and ampicillin were from Fisher Scientific (Fair Lawn,
137 NJ). Restriction digestion enzymes *Hind* III, *Eco*RI, and *Bam*HI were from New England
138 Biolabs (Ipswich, MA). Agarose powder was from Amresco (Atlanta, GA). Polysorbate
139 20, lactose monohydrate, and methanol anhydrate were from Sigma-Aldrich (St. Louis,
140 MO). GeneRuler 1 kb Plus DNA ladder and Quant-iT™ PicoGreen™ dsDNA Assay Kit
141 were from Thermo Scientific (Waltham, MA). Size #3 hydroxypropyl methylcellulose
142 Quali-V-I capsules were from Qualicaps (Whitsett, NC). GFP ELISA kit was from Abcam
143 (Waltham, MA). A549 cells from ATCC (Manassas, VA) were grown in Roswell Park
144 Memorial Institute (RPMI) medium supplemented with 10% (v/v) fetal bovine serum
145 (FBS) and penicillin–streptomycin at final concentrations of 100 U/mL and 100 μ g/mL,
146 respectively. The cell culture reagents including Trypsin-EDTA used in the subculture
147 were all from Gibco (Grand Island, NY).

148

149 *Plasmid Preparation*

150 The pCMV- β or pVectOZ-GFP was transformed into *E. coli* DH5 α under selective
151 growth conditions and then amplified and purified using a plasmid Midiprep kit. Large
152 scale plasmid preparation was performed using plasmid Maxi kit. The plasmid
153 concentration was evaluated using a Nanodrop 2000 from Thermo Scientific.

154

155 *Preparation of Plasmid DNA Dry Powders Using Thin-Film Freezing*

156 To screen for the best dry powder formulation for oral inhalation into the lung, pCMV- β
157 or pVectOZ-GFP with mannitol and leucine (70:30, w/w) as excipients were dissolved in
158 either water, TE buffer, 1,4-dioxane/water (10/90, v/v), or *Tert*-butanol/water (40/60, v/v)
159 at various solid contents and plasmid loading levels as shown in Table 1. The
160 formulations were temporarily stored in a refrigerator at $\sim 4^{\circ}\text{C}$ before being applied to the
161 TFF process.

162
163 The TFF process and lyophilization were done as previously described [32, 34, 36, 37].
164 Briefly, 0.25 mL of sample was dropped through a 21-gauge syringe dropwise onto a
165 rotating cryogenically cooled stainless-steel surface (-80°C). To form frozen thin films,
166 the speed at which the surface of the drum rotated was controlled at 5–7 rpm to avoid
167 the overlap of droplets. The frozen thin films were removed using a steel blade and
168 collected in liquid nitrogen in a glass vial. The glass vial was capped with a rubber
169 stopper with half open and transferred into a -80°C freezer for a temporary storage, and
170 then transferred to a VirTis Advantage bench top tray lyophilizer with stopper re-cap
171 function (The VirTis Company, Inc. Gardiner, NY). Lyophilization was performed over 60
172 h at pressures no more than 100 mTorr, while the shelf temperature was gradually
173 ramped from -40°C to 25°C . The lyophilization cycle is shown in Table 2.

174

175 *In Vitro Aerosol Performance Evaluation*

176 The aerosol performance properties of the thin-film freeze-dried (TFFD) plasmid
177 powders were determined as previously described [32, 34, 36, 37]. Briefly, a Next
178 Generation Pharmaceutical Impactor (NGI) (MSP Corp, Shoreview, MN) connected to a
179 High-Capacity Pump (model HCP5, Copley Scientific, Nottingham, UK) and a Critical
180 Flow Controller (model TPK 2000, Copley Scientific, Nottingham, UK) was adopted to
181 assess the aerosol performance. To avoid bounce of emitted particles across NGI
182 collection plates, the plates were precoated with 1.5%, w/v, polysorbate 20 in methanol
183 and dried in air before use. Plasmid DNA powder (2–3 mg) was loaded into a Size #3
184 capsule, and the capsule was loaded into a high-resistance Plastiap[®] RS00 inhaler
185 (Plastiap S.p.A, Osnago, Italy) attached to a United States Pharmacopeia (USP)
186 induction port (Copley Scientific, Nottingham, UK). The powder was dispersed to the

187 NGI at the flow rate of 60 L/min for 4 s per actuation, providing a 4 kPa pressure drop
188 across the device. Then, the powders in the capsule, inhaler, adapter, induction port,
189 stages 1–7, and the micro-orifice collector (MOC) were collected by dissolving them
190 with water, and the amount of plasmid DNA in samples was quantified using a
191 PicoGreen™ dsDNA Assay Kit following the manufacturer's instruction.

192

193 The Copley Inhaler Testing Data Analysis Software (CITDAS) Version 3.10 (Copley
194 Scientific, Nottingham, UK) was used to calculate the MMAD, the geometric standard
195 deviation (GSD), and the FPF values. The FPF of recovered dose was calculated as the
196 total amount of plasmid collected with an aerodynamic diameter below 5 µm as a
197 percentage of the total amount of plasmid collected. The FPF of delivered dose was
198 calculated as the total amount of plasmids collected with an aerodynamic diameter
199 below 5 µm as a percentage of the total amount plasmids deposited on the adapter, the
200 induction port, stages 1–7 and MOC of the NGI device.

201

202 *Scanning Electron Microscopy (SEM)*

203 The morphology of powder was examined using a Zeiss Supra 40C scanning electron
204 microscope (Carl Zeiss, Heidenheim an der Brenz, Germany) in the Institute for Cell
205 and Molecular Biology Microscopy and Imaging Facility at The University of Texas at
206 Austin. A small amount of bulk powder (i.e., a flake of TFF powder) was deposited on
207 the specimen stub using a double-stick carbon tape. A sputter was used to coat the
208 sample with 15 nm of 60/40 of Pd/Pt before capturing images.

209

210 *Moisture Content Measurement*

211 TFF powder (10 mg, n = 3) was diluted into CombiMethanol solvent from Aquastar
212 (Darmstadt, Germany), and the moisture was measured and determined using a Mettler
213 Toledo V20 volumetric Karl Fischer (KF) titrator (Columbus, OH).

214

215 *X-ray Powder Diffraction (XRPD)*

216 A Rigaku Miniflex 600 II (Rigaku, Tokyo, Japan) equipped with primary monochromated
217 radiation (Cu K radiation source, $\lambda = 1.54056 \text{ \AA}$) was adopted for XRPD study. Plasmid

218 pCMV- β powder sample was loaded onto the sample holder and then analyzed in
219 continuous mode. The operating conditions of accelerating voltage of 40 kV was at 15
220 mA, step size of 0.02° over a 2 θ range of 5-40°, scan speed of 1°/min, and dwell time of
221 2 s as previously described [26].

222

223 *Modulated Differential Scanning Calorimetry (mDSC)*

224 Plasmid pCMV- β powder (3-5 mg) was accurately weighed and loaded into Tzero
225 aluminum hermetic crucibles. A puncture was made in the top lid, right before the DSC
226 measurement. A Model Q20 (TA Instruments, New Castle, DE) differential scanning
227 calorimeter equipped with a refrigerated cooling system (RCS40, TA Instruments, New
228 Castle, DE) was used. In the measurement process, samples were first cooled down to
229 -40°C at a rate of 10°C/min and then ramped up from -40 to 300°C at a rate of 5°C/min.
230 The rate of dry nitrogen gas flow was set as 50 mL/min. The scans were performed with
231 a modulation period of 60 s and a modulated amplitude of 1°C. A TA Instruments Trios
232 v.5.1.1.46572 software was used to analyze the data.

233

234 *Restriction Digestion and Agarose Gel Electrophoresis*

235 Plasmid pCMV- β or pVectOZ-GFP was formulated into formulation P7 (see Table 1)
236 and thin-film freeze-dried. The pCMV- β powder was reconstituted and then digested
237 with *EcoR* I alone or *Hind* III and *EcoR* I for 2 h at 37°C. The pVectOZ-GFP plasmid dry
238 powder was reconstituted and then digested with *Hind* III alone or both *Hind* III and
239 *Bam*HI for 2 h at 37°C. Final restriction digestion products were applied to agarose gel
240 (0.8%) for electrophoresis. Controls include plasmid alone or plasmid in formulation P7
241 without being subjected to TFFD, both restriction-digested before electrophoresis.

242

243 *In Vitro Transfection Study with A549 Cells*

244 A549 cells were seeded in a 24-well plate (2.1 x 10⁵/well) and incubated at 37°C, 5%
245 CO₂. An 80% of confluence was reached after 24 h. To prepare the cell transfection
246 reagents, pVectOZ-GFP in formulation P7 before and after being subjected to TFF (i.e.,
247 dry powder reconstituted with water) was mixed with Lipofectamine 3000 following the
248 manufacturer's instruction. Cells were treated with the reagent (amount fixed) mixed

249 with 100, 250, 500, 1000 and 2500 ng of pDNA/well in formulation P7 before being
250 subjected to TFF to determine the optimum dose for cell transfection, and 500 ng of
251 pDNA/well was selected to compare GFP expression by pVectOZ-GFP before and after
252 being subjected to TFF. The cell medium was changed to fresh medium after 20 h, and
253 cells were then incubated for another 24 h. Finally, cells were washed with 1 × PBS,
254 harvested, and suspended in a cell lysis buffer for 30 min. The supernatant was
255 collected and measured with a GFP ELISA kit following the manufacturer's instruction.
256 Controls include Lipofectamine 3000 alone and cells left untreated.

257

258 *Spray Freezing and Spray Freeze-Drying*

259 Plasmid pCMV-β in formulation 7 (Table 1) were spray-atomized using a 2-fluid nozzle
260 (BUCHI Corporation, DE, New Castle) at different air-flow rates (20, 15, 5 or 2.5 L/min)
261 with high purity nitrogen. The air-flow rate was controlled via a critical flow controller
262 (TPK 2000, Copley Scientific, Nottingham, UK) positioned at the nozzle input. The
263 resultant droplets with a diameter ranging from 30-50 μm were atomized into a liquid
264 nitrogen containing Erlenmeyer flask submerged in liquid nitrogen. The resultant frozen
265 material containing flask was placed in a -80°C freezer to allow the liquid nitrogen to
266 evaporate and thawed at 4°C for agarose gel electrophoresis. For spray freeze-drying,
267 the spray-frozen material was dried in a bench lyophilizer following the drying
268 procedures shown in Table 2.

269

270

271

272

273

274

275

276

277

278

279

280 RESULTS AND DISCUSSION

281

282 *In Vitro Aerosol Performance*

283 The aerosol performance properties of the TFF pDNA powders are shown in Fig. 1 and
284 Table 3. Overall, all nine powders showed good aerosol properties. However, it is also
285 clear that dry powders prepared with lower solid contents showed better aerosol
286 performance. For example, the $FPF_{<5 \mu m}$ values (of the delivered dose) of the plasmid
287 formulations prepared with 1.0, 0.5 and 0.25%, w/v, of solid content (i.e., P1, P4 and
288 P3) were $57.26 \pm 3.19\%$, $56.63 \pm 3.82\%$ and $72.32 \pm 0.41\%$, respectively, and the
289 MMAD values of these powders were $1.58 \pm 0.07 \mu m$, $1.77 \pm 0.22 \mu m$ and 1.44 ± 0.16
290 μm , respectively (Table 3 and Fig. 2A). As to the effect of the plasmid loading (i.e.,
291 plasmid weight vs. total weight) on the aerosol performance, lower plasmid loading
292 showed better aerosol performance. For example, the $FPF_{<5 \mu m}$ values (of the delivered
293 dose) of plasmid formulations prepared with 10.0, 5.0 and 2.5%, w/w, of plasmid (i.e.,
294 P5, P3 and P6, respectively) were $46.16 \pm 4.44\%$, $72.32 \pm 0.41\%$ and $80.39 \pm 3.23\%$,
295 respectively, and the MMAD values of these powders were $1.69 \pm 0.30 \mu m$, 1.44 ± 0.16
296 μm and $1.27 \pm 0.40 \mu m$, respectively (Table 3 and Fig. 2B). This was likely due to the
297 polymeric nature of plasmid DNA. At higher plasmid loading (e.g., 10% vs. 2.5%),
298 stronger intermolecular interactions may have made the powders more difficult to break
299 when they were actuated from the DPI device.

300

301 The effects of co-solvent and TE buffer on the aerosol performance were also
302 investigated. TE buffer was included with the intention to protect pDNA from DNase
303 digestion as the EDTA in the TE buffer is a chelator of divalent cations such as Mg^{2+} ,
304 which are required for the DNase activity [38]. The 1,4-dioxane and *Tert*-butanol were
305 used to prepare cosolvents because data from our previous studies showed that they
306 help increase the solubility of certain molecules in water and improve the aerosol
307 properties of the resultant TFF powders [37]. Overall, including TE buffer, 1,4-dioxane,
308 or *Tert*-butanol in the solvent did not improve the $FPF_{<5 \mu m}$ (Fig. 1, Table 3). It appeared
309 that including the TE buffer in the solvent led to a slight decrease in the aerosol
310 performance properties of the resultant dry powder (i.e., P3 vs. P7, Fig. 1 and Table 3).

311 If the stability of the pDNA during long term storage needs improvement, then the TE
312 buffer or EDTA alone may be included in the powder. The slightly negative effect of the
313 1,4-dioxane/water or t-butanol/water cosolvents on the aerosol performance of the
314 resultant pDNA powders may be attributed to the highly water-soluble nature of the
315 pDNA. Ultimately, formulations P3 and P7 were chosen for additional characterization
316 because they both have desirable aerosol properties and contained a relatively high
317 amount of the pDNA (i.e., 5% pDNA loading).

318

319 *Physical Characteristics of Thin-Film Freeze-Dried Plasmid DNA Powders*

320 The moisture content in the pDNA powder formulation P3 was $1.59 \pm 0.12\%$ (w/w). SEM
321 images revealed that the pDNA powder formulation P3 contained nanostructured
322 aggregates (Fig. 3A-B), with highly porous matrix structure (Fig. 3C), which explains the
323 good aerosol performance properties of the powder as shown in Fig. 1 and Table 3.

324

325 XRPD and DSC were carried out to analyze pDNA powder formulation 7. XRPD
326 diffractogram (Fig. 4) showed that TE salt was in crystalline form after the TFF process
327 as several sharp peaks were observed in the TFF neat TE salts (e.g., 10.8, 14, 15.2, 18.2,
328 20.2, 21.5, 22.5, 23.5, 26, 27, 27.5, 31, 32.2, 33, 34, and 39.2-degree two-theta) and TFF
329 pDNA P7 formulation (e.g., 10.8 and 15.2 degree two-theta). Sharp peaks of mannitol
330 were observed in TFF neat mannitol (e.g., 9.5, 13.5, 14.5, 17, 18.5, 20.2, 21, 22, 24.5, 25,
331 27.5, and 36 degree two-theta), TFF mannitol and leucine (e.g., 9.5, 20.2, 21, 24.5, 25,
332 and 36 degree two-theta), and TFF pDNA formulation (e.g., 9.5, 20.2, 21, 24.5, 25, and
333 36 degree two-theta). The XRPD peak patterns of mannitol in these samples
334 demonstrated that mannitol remained crystalline as a mixture of the δ and α forms [39].
335 Similarly, some peaks of leucine (e.g., 6 and 19 degree two-theta) were observed in the
336 TFF neat leucine, TFF mannitol and leucine, and the TFF pDNA formulation, indicating
337 that leucine remained crystalline after the process.

338

339 DSC was also used to determine the physical state of pDNA powder and excipients. The
340 melting points of Tris and EDTA disodium salt were reported to be $\sim 175^\circ\text{C}$ [40] and
341 $\sim 242^\circ\text{C}$ [41], respectively. Although XRPD diffractograms clearly demonstrated that Tris

342 and EDTA disodium were crystalline after the process, no clear endothermic peak of Tris
343 and EDTA disodium was observed on the DSC thermograms (Fig. 5, black line). Since
344 both salts generally undergo thermal decomposition after melting [42], it is possible that
345 the melting point of Tris and EDTA disodium was interfered by thermal decomposition.
346 DSC thermograms showed that the melting point of TFF neat leucine and TFF neat
347 mannitol was about 274°C and 167°C, respectively (purple and blue line). In the presence
348 of mannitol, the melting point of leucine was decreased to 213°C (green line). Additionally,
349 the melting point of leucine in TFF leucine and TE salt was further decreased to 197°C
350 (yellow line), indicating that the presence of TE salt also contributed to the melting point
351 depression of leucine. Although the presence of leucine did not result in the melting point
352 depression of mannitol (~166°C), the melting point of mannitol decreased to ~135°C
353 (orange line) when TE salt was combined with mannitol. Comparing DSC thermograms
354 in the red and pink lines, the addition of pDNA in the formulation slightly decreased the
355 melting point of mannitol and leucine (~129°C and ~216°C, respectively). No melting or
356 glass transition temperature of pDNA was observed in the TFF pDNA formulation P7.
357 Since the pDNA loading was only 5% in the formulation, the thermal events of pDNA were
358 possibly below the detection limit of DSC analysis [43]. Finally, it is noted that both XRPD
359 and DSC analyses were done using TFF pDNA powder formulation 7 that contained TE
360 buffer. TFF pDNA powder formulation 3 that did not contain TE buffer was not analyzed,
361 but data from our previously studies showed that TFF processed mannitol/leucine
362 mixtures are crystalline as well [29, 44].

363

364 *Integrity of Plasmid DNA After Being Subject to Thin-Film Freezing*

365 Plasmid powder formulation P7 had 5% pDNA loading, contained TE, and showed
366 overall good aerosol performance properties. It was therefore chosen to test the
367 integrity of the pDNA after it was subjected to TFF and reconstitution. As shown in Fig.
368 6, subjecting pCMV- β to TFF did not cause any significant change in the plasmid when
369 comparing the plasmid before being subjected to TFF and reconstitution, with or without
370 restriction digestion, in the agarose gel electrophoresis image, demonstrating that the
371 TFF process did not compromise the chemical integrity of the plasmid.

372

373 *In Vitro Cell Transfection Study*

374 To further investigate the integrity of the pDNA after being subjected to TFF, the pDNA's
375 ability to transfect cells was tested in cells in culture. To do this, pVectOZ-GFP that
376 expresses GFP protein was complexed with Lipofectamine-3000 to transfect A549
377 human lung epithelium cells. Agarose gel electrophoresis and restriction digestion with
378 *Hind* III alone or *Hind* III and *Bam* H1 confirmed the integrity of the plasmid after it was
379 subjected to TFF (data not shown). To optimize the pDNA dose in the *in vitro* cell
380 transfection study, the effect of the pDNA dose on GFP expression in A549 cells was
381 studied. As shown in Fig. 7A, overall, increasing plasmid dose led to higher levels of
382 GFP expression; however, at the highest dose tested (i.e., 2000 ng/well), the GFP
383 expression was lower than at 1000 ng/well. At all doses tested, no apparent cell toxicity
384 was observed, likely because the dose of Lipofectamine was kept constant. The excess
385 plasmids in the 2000 ng/well group may have contributed to the reduced GFP
386 expression; when the ratio of the plasmid to the Lipofectamine was too high, the
387 resultant complexes may not be readily taken up by the cells. Nonetheless, the 500
388 ng/well dose was chosen to test the transfection efficiency of the pVectOZ-GFP before
389 and after being subjected to TFF, and data in Fig. 7B showed that the TFF process did
390 not significantly affect the activity of the plasmid, as there was not any difference in the
391 GFP expression levels before and after TFF.

392

393 *Plasmid DNA Integrity After Actuation Using a Dry Powder Inhaler*

394 The shear stress generated by nebulizing pDNA in liquid is known to cause damage to
395 pDNA and can significantly reduce its transfection efficiency [8-10, 12]. Therefore, we
396 investigated whether aerosolization of the TFF processed pDNA powder with a DPI
397 device causes damage to pDNA. The pCMV- β plasmid was chosen in this study due to
398 its larger size (i.e., 7.2k bp). We tested the integrity of pCMV- β after it was subjected to
399 TFF and then aerosolized using a PlastiTap NGI device. As positive controls, the pDNA
400 in a solution that contained the identical excipients as in the powder was subjected to
401 spray freezing or spray freeze-drying, as spraying is known to damage pDNA [13-16].
402 As shown in Fig. 8, no significant plasmid configuration change (e.g., nicking or linear
403 form) was detectable after the plasmid was subjected to TFF (Lane 2 vs. Lane 3) and

404 after the TFF pDNA powder was actuated from an DPI into NGI (Lane 2 vs. Lane 4),
405 indicating that the plasmid would not be damaged when aerosolized as TFF powders
406 using a DPI device into human lungs.

407

408 On the contrary, spray freezing at different air-flow rates (i.e., 20-2.5 L/min) caused
409 changes in the plasmid (e.g., nicking as shown in Fig. 8, Lane 5, or various levels of
410 linearization as shown in Lanes 6-8). The damages to the plasmid were likely from the
411 shear stress during the spraying as pDNA is routinely subjected to freezing for longer
412 term storage. Compared to spray freezing alone, spray freeze-drying showed a
413 significant increase of linear and nicked forms of the plasmid (Fig. 8, Lanes 8 vs. 9),
414 indicating the damages to the plasmid induced by the shear stress during the spray
415 freezing step was amplified during the drying process. The finding is in agreement with
416 reports by others showing the effect of shear stress during spray drying and spray
417 freeze-drying on pDNA integrity. To overcome the damages caused the shearing,
418 plasmids are often complexed with cationic polymers such as chitosan and
419 polyethyleneimine (PEI), cationic liposomes or nanoparticles, or even encapsulated
420 inside particulates such as poly lactic-co-glycolic acid microparticles [13, 15, 16, 45-47].
421 Unfortunately, those excipients and carriers are often associated with issues such as
422 toxicities that limit their applications in humans [48, 49]. It is noted that cellular uptake of
423 naked pDNA in its native form is relatively inefficient [50, 51], and complexing pDNA
424 with cationic polymers or liposomes are usually employed to promote cellular uptake of
425 pDNA [50, 52, 53]. Nonetheless, there is evidence that when naked pDNA is delivered
426 into the lung of animals such as sheep, specific immune response against the antigens
427 encoded by the plasmid can be induced [54, 55].

428

429

430

431

432

433

434

435 **CONCLUSION**

436 It is feasible to apply TFF technology to engineer dry powders of pDNA with desirable
437 aerosol performance, while preserving the chemical integrity and activity of the pDNA.
438 In addition, the plasmid DNA in the dry powders is not sensitive to shearing when
439 actuated using a dry powder inhaler.

440

441

442 **ACKNOWLEDGEMENT**

443 Cui and Williams report financial support from TFF Pharmaceuticals, Inc.

444

445

446 **DISCLOSURE OF CONFLICT OF INTEREST**

447 Cui reports a relationship with TFF Pharmaceuticals, Inc. that includes equity or stocks
448 and research funding. Williams reports a relationship with TFF Pharmaceuticals, Inc.
449 that includes consulting or advisory, equity or stocks, and research funding. Xu and
450 Moon report a relationship with TFF Pharmaceuticals, Inc. that includes: consulting or
451 advisory. Financial conflict of interest management plans are available at UT Austin.

452

453

454

455

456

457

458

459

460

461

462

463

464

465

466 **REFERENCES**

467

- 468 1. Forde, G.M., *Rapid-response vaccines—does DNA offer a solution?* Nature
469 biotechnology, 2005. **23**(9): p. 1059-1062.
- 470 2. Birchall, J., *Pulmonary delivery of nucleic acids*. Expert opinion on drug delivery,
471 2007. **4**(6): p. 575-578.
- 472 3. Giudice, E.L. and J.D. Campbell, *Needle-free vaccine delivery*. Advanced drug
473 delivery reviews, 2006. **58**(1): p. 68-89.
- 474 4. Simonsen, L., et al., *Unsafe injections in the developing world and transmission
475 of bloodborne pathogens: a review*. Bulletin of the World Health Organization,
476 1999. **77**(10): p. 789.
- 477 5. West, J. and D.M. Rodman, *Gene therapy for pulmonary diseases*. Chest, 2001.
478 **119**(2): p. 613-617.
- 479 6. Vachani, A., et al., *Gene therapy for mesothelioma and lung cancer*. American
480 journal of respiratory cell and molecular biology, 2010. **42**(4): p. 385-393.
- 481 7. Lu, D. and A.J. Hickey, *Pulmonary vaccine delivery*. Expert review of vaccines,
482 2007. **6**(2): p. 213-226.
- 483 8. Catanese, D., et al., *Supercoiled Minivector DNA resists shear forces associated
484 with gene therapy delivery*. Gene therapy, 2012. **19**(1): p. 94-100.
- 485 9. Arulmuthu, E.R., et al., *Studies on aerosol delivery of plasmid DNA using a mesh
486 nebulizer*. Biotechnology and bioengineering, 2007. **98**(5): p. 939-955.
- 487 10. Lentz, Y., T. Anchordoquy, and C. Lengsfeld, *DNA acts as a nucleation site for
488 transient cavitation in the ultrasonic nebulizer*. Journal of pharmaceutical
489 sciences, 2006. **95**(3): p. 607-619.
- 490 11. Levy, M.S., et al., *Biochemical engineering approaches to the challenges of
491 producing pure plasmid DNA*. Trends in biotechnology, 2000. **18**(7): p. 296-305.
- 492 12. Birchall, J.C., I.W. Kellaway, and M. Gumbleton, *Physical stability and in-vitro
493 gene expression efficiency of nebulised lipid-peptide-DNA complexes*.
494 International journal of pharmaceuticals, 2000. **197**(1-2): p. 221-231.
- 495 13. Mohri, K., et al., *Optimized pulmonary gene transfection in mice by spray-freeze
496 dried powder inhalation*. Journal of Controlled Release, 2010. **144**(2): p. 221-226.
- 497 14. Lengsfeld, C. and T. Anchordoquy, *Shear-induced degradation of plasmid DNA*.
498 Journal of pharmaceutical sciences, 2002. **91**(7): p. 1581-1589.
- 499 15. Kuo, J.h.S., *The effect of protective agents on the stability of plasmid DNA by the
500 process of spray-drying*. Journal of pharmacy and pharmacology, 2003. **55**(3): p.
501 301-306.
- 502 16. Kuo, J.h.S. and R. Hwang, *Preparation of DNA dry powder for non-viral gene
503 delivery by spray-freeze drying: effect of protective agents (polyethyleneimine
504 and sugars) on the stability of DNA*. Journal of Pharmacy and Pharmacology,
505 2004. **56**(1): p. 27-33.
- 506 17. Overhoff, K.A., et al., *Use of thin film freezing to enable drug delivery: a review*.
507 Journal of Drug Delivery Science and Technology, 2009. **19**(2): p. 89-98.
- 508 18. Overhoff, K.A., et al., *Novel ultra-rapid freezing particle engineering process for
509 enhancement of dissolution rates of poorly water-soluble drugs*. European journal
510 of pharmaceuticals and biopharmaceutics, 2007. **65**(1): p. 57-67.

- 511 19. Alzhrani, R.F., et al., *Thin-Film Freeze-Drying Is a Viable Method to Convert*
512 *Vaccines Containing Aluminum Salts from Liquid to Dry Powder*, in *Vaccine*
513 *Delivery Technology*. 2020, Springer. p. 489-498.
- 514 20. Sahakijpijarn, S., et al., *A Safety and Tolerability Study of Thin Film Freeze-Dried*
515 *Tacrolimus for Local Pulmonary Drug Delivery in Human Subjects*.
516 *Pharmaceutics*, 2021. **13**(5): p. 717.
- 517 21. Sahakijpijarn, S., et al., *Using thin film freezing to minimize excipients in*
518 *inhalable tacrolimus dry powder formulations*. *Int J Pharm*, 2020. **586**: p. 119490.
- 519 22. Sahakijpijarn, S., et al., *Development of Remdesivir as a Dry Powder for*
520 *Inhalation by Thin Film Freezing*. *Pharmaceutics*, 2020. **12**(11).
- 521 23. Moon, C., et al., *Enhanced Aerosolization of High Potency Nanoaggregates of*
522 *Voriconazole by Dry Powder Inhalation*. *Mol Pharm*, 2019. **16**(5): p. 1799-1812.
- 523 24. Moon, C., et al., *Processing design space is critical for voriconazole*
524 *nanoaggregates for dry powder inhalation produced by thin film freezing*. *Journal*
525 *of Drug Delivery Science and Technology*, 2019. **54**.
- 526 25. Jara, M.O., et al., *Niclosamide Inhalation Powder Made by Thin-Film Freezing:*
527 *Pharmacokinetic and Toxicology Studies in Rats and Hamsters*. bioRxiv, 2021.
- 528 26. Hufnagel, S., et al., *Dry Powders for Inhalation Containing Monoclonal Antibodies*
529 *Made by Thin-Film Freeze-Drying*. *International Journal of Pharmaceutics*, 2022:
530 p. 121637.
- 531 27. AboulFotouh, K., et al., *Development of (Inhalable) Dry Powder Formulations of*
532 *AS01B-Containing Vaccines Using Thin-Film Freeze-Drying*. *International*
533 *Journal of Pharmaceutics*, 2022: p. 121825.
- 534 28. AboulFotouh, K., et al., *Formulation of dry powders of vaccines containing MF59*
535 *or AddaVax by Thin-Film Freeze-Drying: Towards a dry powder universal flu*
536 *vaccine*. *International Journal of Pharmaceutics*, 2022. **624**: p. 122021.
- 537 29. Wang, J.-L., et al., *Aerosolizable siRNA-Encapsulated Solid Lipid Nanoparticles*
538 *Prepared by Thin-film Freeze-Drying for Potential Pulmonary Delivery*.
539 *International Journal of Pharmaceutics*, 2021: p. 120215.
- 540 30. Thakkar, S.G., et al., *Intranasal immunization with aluminum salt-adjuvanted dry*
541 *powder vaccine*. *Journal of Controlled Release*, 2018. **292**: p. 111-118.
- 542 31. Thakkar, S.G., et al., *The immunogenicity of thin-film freeze-dried, aluminum salt-*
543 *adjuvanted vaccine when exposed to different temperatures*. *Human Vaccines &*
544 *Immunotherapeutics*, 2017: p. 1-11.
- 545 32. Li, X., et al., *A method of lyophilizing vaccines containing aluminum salts into a*
546 *dry powder without causing particle aggregation or decreasing the*
547 *immunogenicity following reconstitution*. *J Control Release*, 2015. **204**: p. 38-50.
- 548 33. Dao, H.M., et al., *Aggregation of Lactoferrin Caused by Droplet Atomization*
549 *Process via a Two-Fluid Nozzle: The Detrimental Effect of Air–Water Interfaces*.
550 *Molecular Pharmaceutics*, 2022. **19**(7): p. 2662-2675.
- 551 34. Sahakijpijarn, S., et al., *Development of remdesivir as a dry powder for inhalation*
552 *by thin film freezing*. *Pharmaceutics*, 2020. **12**(11): p. 1002.
- 553 35. MacGregor, G.R. and C.T. Caskey, *Construction of plasmids that express E. coli*
554 *beta-galactosidase in mammalian cells*. *Nucleic Acids Research*, 1989. **17**(6): p.
555 2365.

- 556 36. Sahakijpiparn, S., et al., *Using thin film freezing to minimize excipients in*
557 *inhalable tacrolimus dry powder formulations*. International Journal of
558 Pharmaceutics, 2020. **586**: p. 119490.
- 559 37. Moon, C., et al., *Processing design space is critical for voriconazole*
560 *nanoaggregates for dry powder inhalation produced by thin film freezing*. Journal
561 of Drug Delivery Science and Technology, 2019. **54**: p. 101295.
- 562 38. Murakami, M., *Evaluation of DNA plasmid storage conditions*. The Open
563 Biotechnology Journal, 2013. **7**(1).
- 564 39. Cares-Pacheco, M., et al., *Physicochemical characterization of D-mannitol*
565 *polymorphs: the challenging surface energy determination by inverse gas*
566 *chromatography in the infinite dilution region*. International journal of
567 pharmaceutics, 2014. **475**(1-2): p. 69-81.
- 568 40. Medicine, N.L.o., *Compound summary*
569 <https://pubchem.ncbi.nlm.nih.gov/compound/Tromethamine>. 2005.
- 570 41. *Compound summary* [https://pubchem.ncbi.nlm.nih.gov/compound/EDTA-](https://pubchem.ncbi.nlm.nih.gov/compound/EDTA-disodium-salt#section=Color-Form)
571 [disodium-salt#section=Color-Form](https://pubchem.ncbi.nlm.nih.gov/compound/EDTA-disodium-salt#section=Color-Form). 2007.
- 572 42. Kondratenko, Y., et al., *Synthesis, structure and properties of tris*
573 *(hydroxymethyl) aminomethane complexes with biogenic metal salts*. Inorganica
574 Chimica Acta, 2022. **530**: p. 120705.
- 575 43. Lappalainen, M. and M. Karppinen, *Techniques of differential scanning*
576 *calorimetry for quantification of low contents of amorphous phases*. Journal of
577 thermal analysis and calorimetry, 2010. **102**(1): p. 171-180.
- 578 44. Sahakijpiparn, S., et al., *In vivo pharmacokinetic study of remdesivir dry powder*
579 *for inhalation in hamsters*. International Journal of Pharmaceutics: X, 2021. **3**: p.
580 100073.
- 581 45. Densmore, C.L., et al., *Aerosol delivery of robust polyethyleneimine–DNA*
582 *complexes for gene therapy and genetic immunization*. Molecular Therapy, 2000.
583 **1**(2): p. 180-188.
- 584 46. Lane, M.E., F.S. Brennan, and O.I. Corrigan, *Comparison of post-emulsification*
585 *freeze drying or spray drying processes for the microencapsulation of plasmid*
586 *DNA*. Journal of pharmacy and pharmacology, 2005. **57**(7): p. 831-838.
- 587 47. Okuda, T., et al., *Development of biodegradable polycation-based inhalable dry*
588 *gene powders by spray freeze drying*. Pharmaceutics, 2015. **7**(3): p. 233-254.
- 589 48. Deng, R., et al., *Revisit the complexation of PEI and DNA—how to make low*
590 *cytotoxic and highly efficient PEI gene transfection non-viral vectors with a*
591 *controllable chain length and structure?* Journal of controlled release, 2009.
592 **140**(1): p. 40-46.
- 593 49. Cortesi, R., et al., *Effect of cationic liposome composition on in vitro cytotoxicity*
594 *and protective effect on carried DNA*. International Journal of Pharmaceutics,
595 1996. **139**(1-2): p. 69-78.
- 596 50. Remaut, K., et al., *Influence of plasmid DNA topology on the transfection*
597 *properties of DOTAP/DOPE lipoplexes*. Journal of controlled release, 2006.
598 **115**(3): p. 335-343.
- 599 51. Zabner, J., et al., *Comparison of DNA-lipid complexes and DNA alone for gene*
600 *transfer to cystic fibrosis airway epithelia in vivo*. The Journal of clinical
601 investigation, 1997. **100**(6): p. 1529-1537.

- 602 52. Jiang, H.-L., et al., *Degradable polyethylenimines as gene carriers*. Materials
603 Science and Technology, 2008. **24**(9): p. 1118-1126.
- 604 53. Davies, L.A., et al., *Enhanced lung gene expression after aerosol delivery of*
605 *concentrated pDNA/PEI complexes*. Molecular Therapy, 2008. **16**(7): p. 1283-
606 1290.
- 607 54. Rajapaksa, A.E., et al., *Effective pulmonary delivery of an aerosolized plasmid*
608 *DNA vaccine via surface acoustic wave nebulization*. Respiratory research, 2014.
609 **15**(1): p. 1-12.
- 610 55. Kodama, Y., et al., *Development of a DNA vaccine for melanoma metastasis by*
611 *inhalation based on an analysis of transgene expression characteristics of naked*
612 *pDNA and a ternary complex in mouse lung tissues*. Pharmaceutics, 2020. **12**(6):
613 p. 540.
614

615

616

617

618

619

620

621

622

623

624

625

626

627

628

629

630

631

632

633

634

635

636

637 **Table 1.** List of plasmid compositions.

Formulation	Plasmid loading (% w/w)	Excipient ratio (w/w)		Solid content (% w/v)	Solvent
		Mannitol	Leucine		
P1	5	7	3	1	Water
P2	10	7	3	1	Water
P3	5	7	3	0.25	Water
P4	5	7	3	0.5	Water
P5	10	7	3	0.25	Water
P6	2.5	7	3	0.25	Water
P7	5	7	3	0.25	TE buffer
P8	5	7	3	0.25	1,4-dioxane/water
P9	5	7	3	0.25	<i>Tert</i> -butanol/water

638

639

640

641

642

643

644

645

646

647

648

649

650

651

652

653

654 **Table 2.** Lyophilization cycle used to dry the thin-film frozen plasmids.

Lyophilization Stage	Parameters
Loading/Freezing temp	-40°C
Primary drying temp	-40°C
Primary drying time	20 h
Ramp to secondary drying	20 h
Secondary drying temp	+25°C
Secondary drying time	20 h

655

656

657

658

659

660

661

662

663

664

665

666

667

668

669

670

671

672

673

674

675

676

677

678

679 **Table 3.** Aerosol performance properties of thin-film freeze-dried pCMV- β powders.
680 Data are mean \pm S.D. ($n = 3$) (MMAD, mass median aerodynamic diameter; GSD,
681 geometric standard deviation; FPF, fine particle fraction).

682

Formulation	MMAD	GSD	FPF (recovered) %	FPF (delivered) %
P1	1.58 \pm 0.07	3.73 \pm 0.67	32.92 \pm 2.52	57.26 \pm 3.19
P2	1.62 \pm 0.10	3.19 \pm 0.29	30.27 \pm 1.12	41.58 \pm 1.80
P3	1.44 \pm 0.16	2.77 \pm 0.19	55.13 \pm 2.36	72.32 \pm 0.41
P4	1.77 \pm 0.22	3.15 \pm 0.21	34.55 \pm 2.34	56.63 \pm 3.82
P5	1.69 \pm 0.30	4.24 \pm 1.38	36.13 \pm 2.53	46.16 \pm 4.44
P6	1.27 \pm 0.40	4.24 \pm 1.38	64.70 \pm 3.53	80.39 \pm 3.23
P7	0.96 \pm 0.05	3.30 \pm 0.67	42.45 \pm 4.73	65.68 \pm 4.12
P8	1.50 \pm 0.15	3.11 \pm 0.54	44.94 \pm 7.27	65.01 \pm 4.22
P9	1.74 \pm 0.19	2.85 \pm 1.20	51.92 \pm 10.52	62.96 \pm 8.86

683

684

685

686

687

688

689

690

691

692

693

694

695

696

697

698 **Figure captions:**

699

700 **Figure 1.** Deposition profiles of TFF plasmid DNA powders in various stages after the
701 powders were applied to NGI using a Plastiape® RS00 high-resistance DPI at a flow
702 rate of 60 L/min. Data are mean \pm S.D. ($n = 3$)

703

704 **Figure 2.** Correlation of solid content (A) and pDNA loading (B) with aerosol
705 performance of TFF plasmid DNA powders. Data are mean \pm S.D. ($n = 3$)

706

707 **Figure 3.** Representative SEM images of a TFF pCMV- β plasmid powder (i.e.,
708 formulation P3).

709

710 **Figure 4.** XRPD diffractograms of TFF pDNA formulation and excipients.

711

712 **Figure 5.** DSC thermograms of TFF pDNA formulation and excipients.

713

714 **Figure 6.** Chemical Integrity of pDNA before and after being subjected to TFF process.

715 Lane 1, undigested pCMV- β in formulation P7 before TFF; Lane 2, pCMV- β in
716 formulation P7 before TFF and digested with *Hind* III and *Eco*RI; Lane 3, pCMV- β in
717 formulation P7 before TFF and digested with *Eco*RI; Lane 4, 1 kb plus DNA ladder;
718 Lane 5, undigested pCMV- β reconstituted from formulation P7 powder; Lane 6, pCMV- β
719 reconstituted from formulation P7 powder and then digested with *Hind* III and *Eco*RI;
720 Lane 7, pCMV- β reconstituted from formulation P7 powder and then digested with
721 *Eco*RI; Lane 8, original unformulated pCMV- β digested with *Hind* III and *Eco*RI; Lane 9,
722 original unformulated pCMV- β digested with *Eco*RI. The loading of plasmid for Lane 1
723 and Lane 5 was 500 ng per well, other lanes were 420 ng.

724

725 **Figure 7.** Cell transfection with pVectOZ-GFP before and after TFF. (A) Optimization of
726 plasmid dose based on the GFP expression levels. (B) GFP expression in A549 cells
727 after transfected with pVectOZ-GFP before and after it was subjected to TFF. Data are
728 mean \pm S.D. ($n = 4$) (n.s., not significant, t-test, two-tail, $p > 0.05$).

729 **Figure 8.** Plasmid DNA integrity after being subjected to TFF, TFF and actuation, spray
730 freezing, and spray freeze-drying (SFD). Lane 1, 1kb plus DNA ladder; Lane 2, pCMV- β
731 in formulation P7 before TFF; Lane 3, pCMV- β reconstituted from formulation P7 TFF
732 powder; Lane 4, pCMV- β in formulation P7 TFF powder collected from NGI plates after
733 the powder was actuated using a DPI; Lanes 5, 6, 7, and 8, pCMV- β in formulation P7
734 after spray freezing at air-flow rate of 20, 15, 5, and 2.4 L/min, respectively; Lane 9,
735 pCMV- β in formulation P7 after SFD at air-flow rate of 15 L/min. The loading of plasmid
736 was 500 ng per lane.

737

738

739

740

741

742

743

744

745

746

747

748

749

750

751

752

753

754

755

756

757

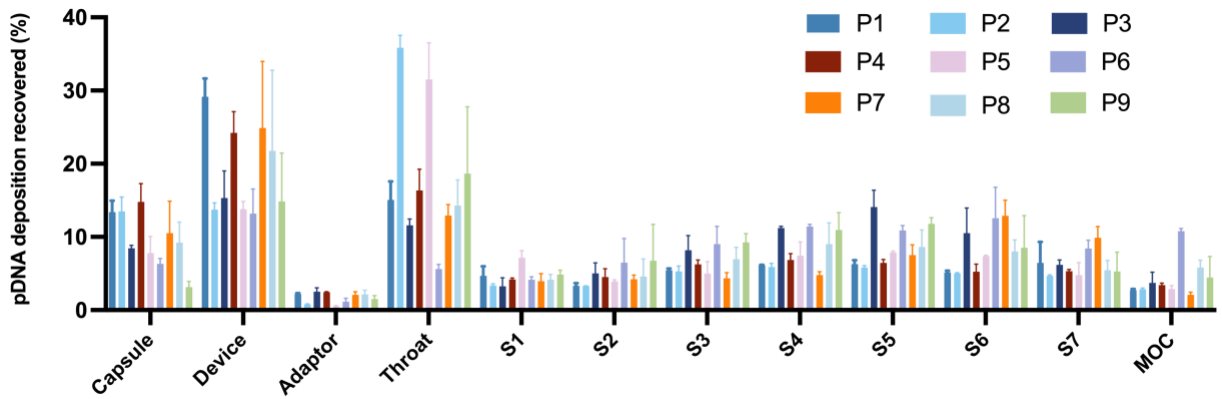
758

759

760

Figure 1.

761



762

763

764

765

766

767

768

769

770

771

772

773

774

775

776

777

778

779

780

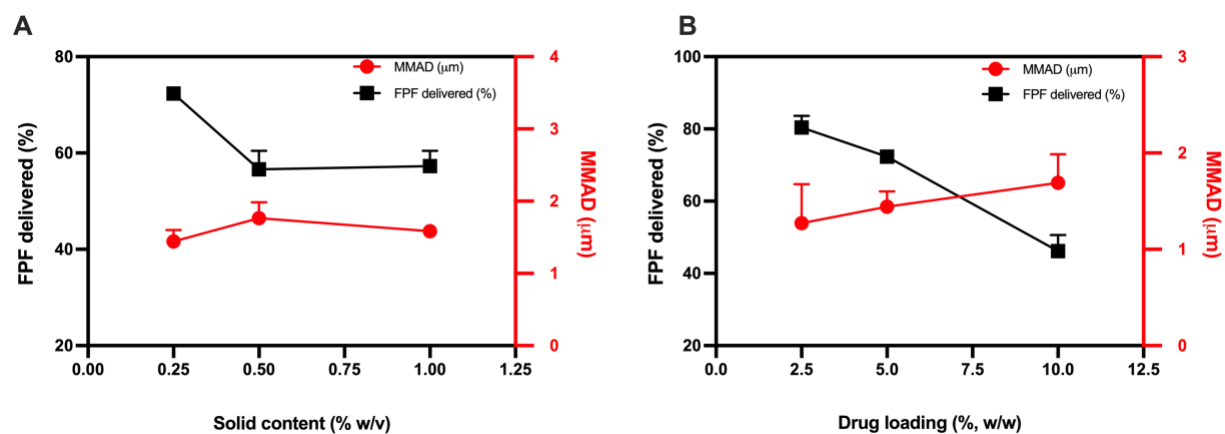
781

782

783

784

Figure 2.



785

786

787

788

789

790

791

792

793

794

795

796

797

798

799

800

801

802

803

804

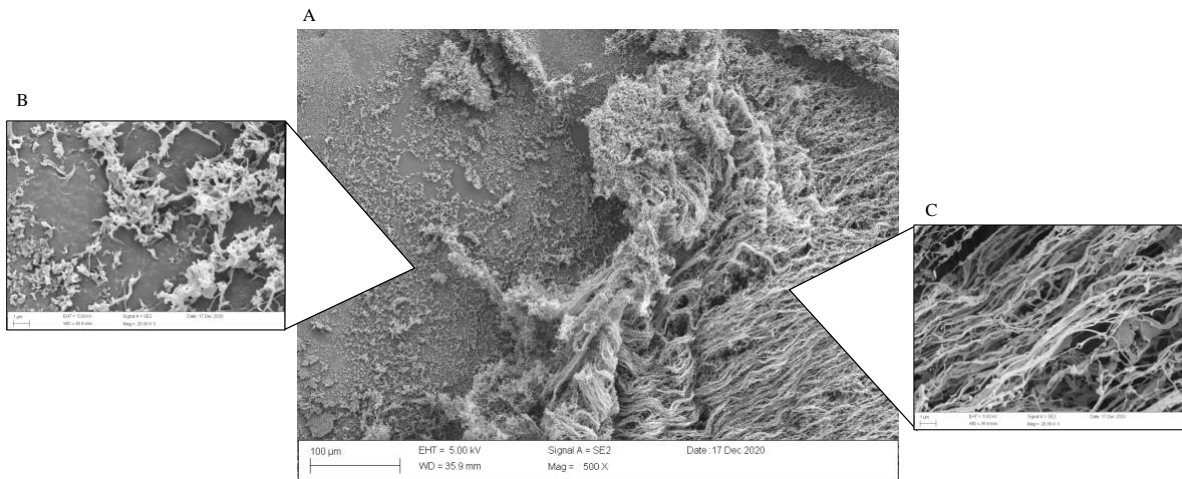
805

806

807

808

Figure 3.



809

810

811

812

813

814

815

816

817

818

819

820

821

822

823

824

825

826

827

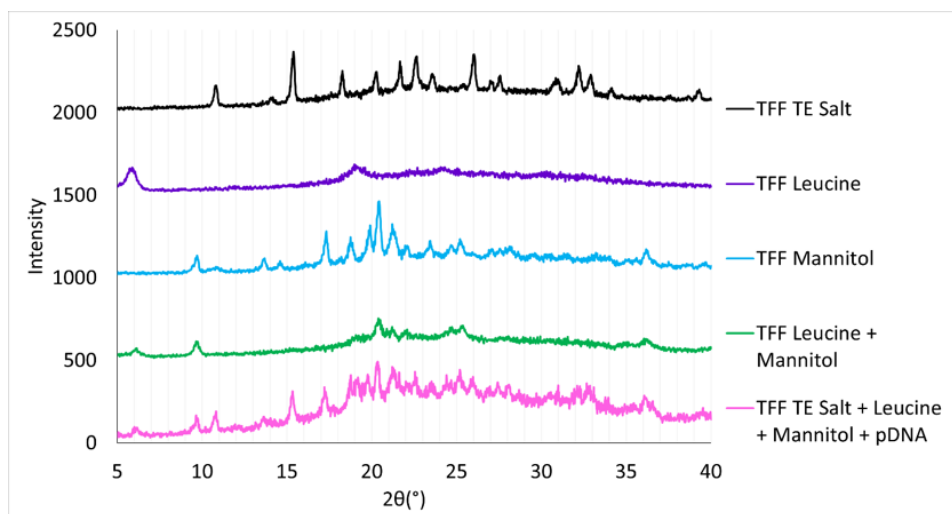
828

829

830

831

Figure 4.



832

833

834

835

836

837

838

839

840

841

842

843

844

845

846

847

848

849

850

851

852

853

854

Figure 5.

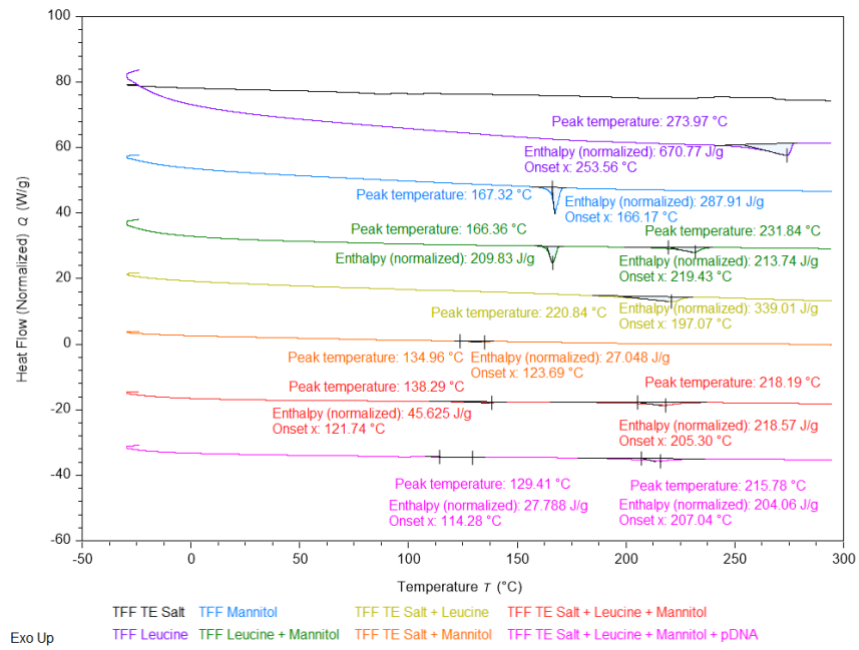
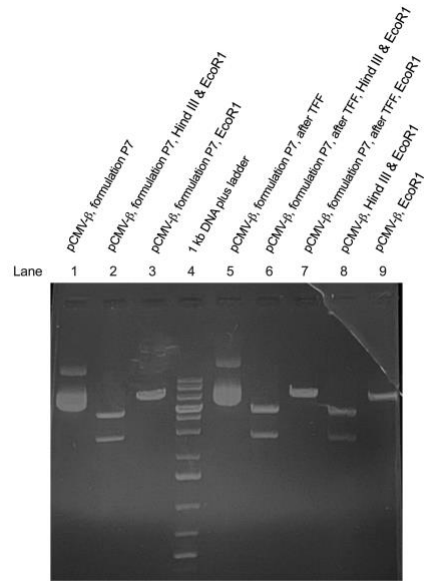


Figure 6.



855

856

857

858

859

860

861

862

863

864

865

866

867

868

869

870

871

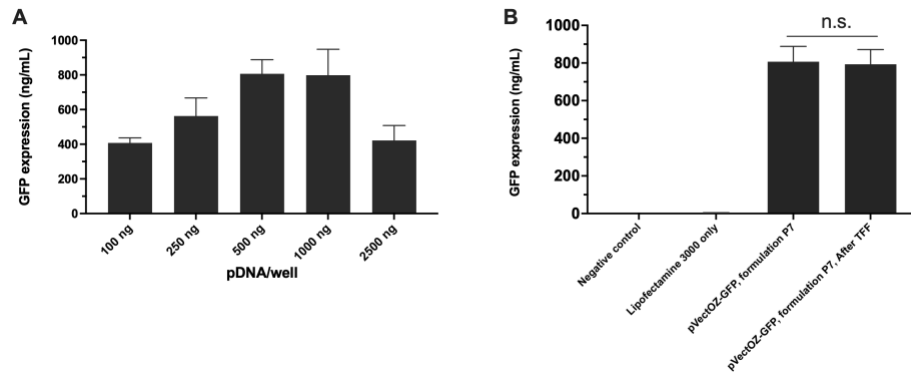
872

873

874

Figure 7.

875



876

877

878

879

880

881

882

883

884

885

886

887

888

889

890

891

892

893

894

895

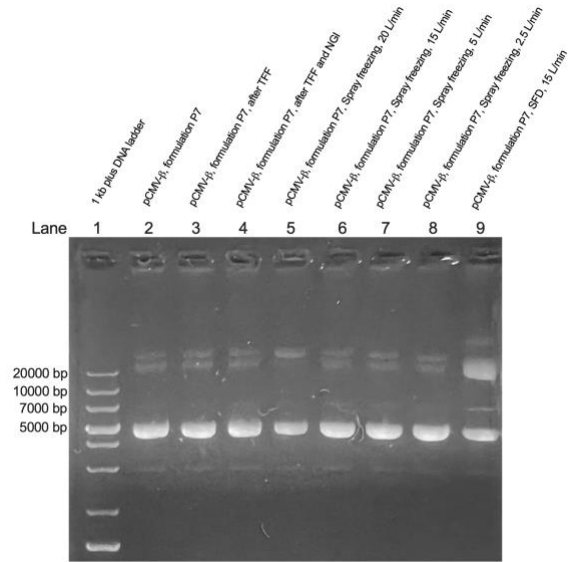
896

897

898

899
900
901

Figure 8.



902